

that is, it is a less strict criterion than homotopic. For analysis of the transfer test data, see Supplementary Information.

Received 8 August 2001; accepted 7 January 2002.

1. Scoville, W. B. & Milner, B. Loss of recent memory after bilateral hippocampal lesions. *J. Neurol. Neurosurg. Psychiatr.* **20**, 11–21 (1957).
2. O'Keefe, J. & Nadel, L. *The Hippocampus as a Cognitive Map* (Clarendon, Oxford, 1978).
3. Squire, L. R. *Memory and Brain* (Oxford Univ. Press, New York, 1987).
4. Cohen, N. J. & Eichenbaum, H. *Memory, Amnesia and the Hippocampal System* (MIT Press, Cambridge, MA, 1993).
5. Bostock, E., Muller, R. U. & Kubie, J. L. Experience-dependent modifications of hippocampal place cell firing. *Hippocampus* **1**, 193–205 (1991).
6. Kentros, C. *et al.* Abolition of long-term stability of new hippocampal place cell maps by NMDA receptor blockade. *Science* **280**, 2121–2126 (1998).
7. Muller, R. U. & Kubie, J. L. The effects of changes in the environment on the spatial firing of hippocampal complex-spike cells. *J. Neurosci.* **7**, 1951–1968 (1987).
8. Wilson, M. A. & McNaughton, B. L. Dynamics of the hippocampal ensemble code for space. *Science* **261**, 1055–1058 (1993).
9. O'Keefe, J. & Speakman, A. Single unit activity in the rat hippocampus during a spatial memory task. *Exp. Brain Res.* **68**, 1–27 (1987).
10. Mehta, M. R., Barnes, C. A. & McNaughton, B. L. Experience-dependent, asymmetric expansion of hippocampal place fields. *Proc. Natl Acad. Sci. USA* **94**, 8918–8921 (1997).
11. Mehta, M. R., Quirk, M. C. & Wilson, M. A. Experience-dependent asymmetric fields. *Neuron* **25**, 707–715 (2000).
12. Jeffery, K. J. in *Neuronal Mechanisms of Memory Formation* (ed. Holscher, C.) 100–121 (Cambridge Univ. Press, Cambridge, 2000).
13. Merzenich, M. M. *et al.* Topographic reorganization of somatosensory cortical areas 3b and 1 in adult monkeys following restricted deafferentation. *Neuroscience* **8**, 33–55 (1983).
14. Clark, S. A., Allard, T., Jenkins, W. J. & Merzenich, M. M. Receptive fields in the body-surface map in adult cortex defined by temporally correlated inputs. *Nature* **332**, 444–445 (1988).
15. Wang, X., Merzenich, M. M., Sameshina, K. & Jenkins, W. M. Remodelling of hand representation in adult cortex determined by timing of tactile stimulation. *Nature* **378**, 71–75 (1995).
16. Weinberger, N. M., Javid, R. & Lapan, B. Long-term retention of learning-induced receptive-field plasticity in the auditory cortex. *Proc. Natl Acad. Sci. USA* **90**, 2394–2398 (1993).
17. O'Keefe, J., Nadel, L., Keightley, S. & Kill, D. Fornix lesions selectively abolish place learning in the rat. *Exp. Neurol.* **48**, 152–166 (1975).
18. Morris, R. G., Garrud, P., Rawlins, J. N. & O'Keefe, J. Place navigation impaired in rats with hippocampal lesions. *Nature* **297**, 681–683 (1982).
19. Sutherland, R. J., Kolb, B. & Whishaw, I. Spatial mapping: definitive disruption by hippocampal or medial frontal cortical damage in the rat. *Neurosci. Lett.* **31**, 271–276 (1982).
20. Barnes, C. A. Spatial learning and memory processes: the search for their neurobiological mechanisms in the rat. *Trends Neurosci.* **11**, 163–169 (1988).
21. O'Keefe, J. & Burgess, N. Geometric determinants of the place fields of hippocampal neurons. *Nature* **381**, 425–428 (1996).
22. Hartley, T., Burgess, N., Lever, C., Cacucci, F. & O'Keefe, J. Modeling place fields in terms of the cortical inputs to the hippocampus. *Hippocampus* **10**, 369–379 (2000).
23. Quirk, G. J., Muller, R. U., Kubie, J. L. & Ranck, J. B. The positional firing properties of medial entorhinal neurons: description and comparison with hippocampal place cells. *J. Neurosci.* **12**, 1945–1963 (1992).
24. Sharp, P. E. Subicular cells generate similar spatial firing patterns in two geometrically and visually distinctive environments: comparison with hippocampal place cells. *Behav. Brain Res.* **85**, 71–92 (1997).
25. Wood, E. R., Dudchenko, P. A. & Eichenbaum, H. The global record of memory in hippocampal neuronal activity. *Nature* **397**, 613–616 (1999).
26. Frank, L. M., Brown, E. M. & Wilson, M. Trajectory encoding in the hippocampus and entorhinal cortex. *Neuron* **27**, 169–178 (2000).
27. Tamila, H., Shapiro, M., Gallagher, M. & Eichenbaum, H. Brain aging: Changes in the nature of information coding by the hippocampus. *J. Neurosci.* **17**, 5155–5166 (1997).
28. Hollup, S. A., Molden, S., Donnett, J. G., Moser, M. B. & Moser, E. I. Accumulation of hippocampal place fields at the goal location in an annular watermaze task. *J. Neurosci.* **21**, 1635–1644 (2001).
29. O'Keefe, J. & Recce, M. L. Phase relationship between hippocampal place units and the EEG theta rhythm. *Hippocampus* **3**, 317–330 (1993).
30. Jeffery, K. J. & O'Keefe, J. Learned interaction of visual and idiothetic cues in the control of place field orientation. *Exp. Brain Res.* **127**, 151–161 (1999).

Supplementary Information accompanies the paper on Nature's website (<http://www.nature.com>).

## Acknowledgements

We thank J. Huxter, T. Hartley and K. Jeffery for discussion, S. Burton for reviewing the manuscript, C. Parker for technical assistance, and J. Donnett for the recording system. This work was supported by a Medical Research Council (UK) programme grant to J.O.K., MRC Advanced Studentships to C.L. and T.W., a Wellcome Trust Studentship to F.C., and Royal Society and MRC Senior Fellowships to N.B.

## Competing interests statement

The authors declare that they have no competing financial interests.

Correspondence and requests for materials should be addressed to C.L. (e-mail: [colin@maze.ucl.ac.uk](mailto:colin@maze.ucl.ac.uk)) or J.O.K. (e-mail: [John@maze.ucl.ac.uk](mailto:John@maze.ucl.ac.uk)).

## Balanced responsiveness to chemoattractants from adjacent zones determines B-cell position

Karin Reif<sup>†</sup>, Eric H. Ekland<sup>†</sup>, Lars Ohl<sup>‡</sup>, Hideki Nakano<sup>§</sup>, Martin Lipp<sup>||</sup>, Reinhold Förster<sup>‡</sup> & Jason G. Cyster<sup>\*</sup>

<sup>\*</sup> Howard Hughes Medical Institute and Department of Microbiology and Immunology, University of California San Francisco, 513 Parnassus Avenue, San Francisco, California 94143-0414, USA

<sup>‡</sup> University Clinic for Surgery, Nikolaus-Fiebiger-Center, 91054 Erlangen, Germany

<sup>§</sup> Department of Immunology, Toho University School of Medicine, Ota-Ku, Tokyo 143-8540, Japan

<sup>||</sup> Molecular Tumorigenetics and Immunogenetics, Max-Delbrück-Center for Molecular Medicine, 13092 Berlin, Germany

<sup>†</sup> These authors contributed equally to this work

B lymphocytes re-circulate between B-cell-rich compartments (follicles or B zones) in secondary lymphoid organs, surveying for antigen. After antigen binding, B cells move to the boundary of B and T zones to interact with T-helper cells<sup>1–3</sup>. Despite the importance of B–T-cell interactions for the induction of antibody responses, the mechanism causing B-cell movement to the T zone has not been defined. Here we show that antigen-engaged B cells have increased expression of CCR7, the receptor for the T-zone chemokines<sup>4,5</sup> CCL19 and CCL21, and that they exhibit increased responsiveness to both chemoattractants. In mice lacking lymphoid CCL19 and CCL21 chemokines, or with B cells that lack CCR7, antigen engagement fails to cause movement to the T zone. Using retroviral-mediated gene transfer we demonstrate that increased expression of CCR7 is sufficient to direct B cells to the T zone. Reciprocally, overexpression of CXCR5, the receptor for the B-zone chemokine CXCL13, is sufficient to overcome antigen-induced B-cell movement to the T zone. These findings define the mechanism of B-cell relocalization in response to antigen, and establish that cell position *in vivo* can be determined by the balance of responsiveness to chemoattractants made in separate but adjacent zones.

Using B cells from mice carrying immunoglobulin transgenes specific for the antigen hen-egg lysozyme (Ig<sup>HEL</sup>)<sup>6</sup> in a time course analysis, we found that movement of antigen-engaged B cells to the B-zone/T-zone (B/T) boundary is complete within 6 h of antigen exposure (Fig. 1a). Antigen-engaged B cells can remain at this location for at least two days<sup>2</sup>, and interactions between T-helper cells and B cells are first observed in this zone<sup>3</sup>. Genetic studies have established that CCR7, and its ligands CCL19 and CCL21, are important for T-cell and dendritic cell localization in T-cell zones<sup>7,8</sup>. To test whether movement of B cells to the T zone might occur owing to increased expression of CCR7, we tested for levels of CCL19-Fc (Fc, fragment crystallizable) binding to antigen-stimulated B cells (Fig. 1b). Six hours after exposure to HEL antigen *in vivo*, Ig<sup>HEL</sup>-transgenic B cells showed a two–threefold increase in binding of CCL19-Fc, and little or no change in CXCR5 expression (Fig. 1b). CCL19-Fc binding to CCR7-deficient B cells was minimal, establishing that CCL19-Fc staining served as a faithful reporter of CCR7 levels (see Supplementary Information). Efforts to measure how the increase in CCR7 affected chemotactic responsiveness of the cells were confounded, as B cells that had bound large amounts of HEL antigen attached irreversibly to transwell filters (data not shown), consistent with reports that HEL binds strongly to many surfaces<sup>9</sup>.

We therefore developed a second approach to study antigen-engaged B-cell redistribution, incubating B cells from IgM<sup>+</sup> con-

genic C57BL/6 (B6) mice *in vitro* with anti-IgM antibody as a surrogate antigen for 1 h, and then transferring the cells to IgM<sup>b</sup> B6 mice. The anti-IgM treatment caused the cells to localize at the B/T boundary (Fig. 1c), and induced upregulation of CCL19-Fc binding, which was equivalent to the induction in HEL binding observed with Ig<sup>HEL</sup>-transgenic B cells (Fig. 1b). *Ex vivo* chemotaxis assays with anti-IgM-stimulated cells revealed an increase in the CCL19 and CCL21 chemokine response profile of the cells, with an increase in the magnitude of the response particularly to low doses of chemokines (Fig. 1d). The basis for the greater augmentation of CCL19 compared with CCL21 responsiveness is unknown. There was no significant change in responsiveness to the B-zone chemo-

kine CXCL13 after B-cell antigen receptor (BCR) stimulation (Fig. 1d), consistent with the lack of change in CXCR5 expression (Fig. 1b).

Our *ex vivo* studies indicated that antigen-mediated relocalization of B cells to the T zone requires B-cell expression of CCR7 and response to the T-zone chemokines CCL19 and CCL21. To test this *in vivo*, we transferred Ig<sup>HEL</sup>-transgenic B cells to *plt/plt* mice that lack the *CCL19* gene<sup>10,11</sup> and the gene for the lymphoid tissue form of *CCL21* (refs 7, 12). In the absence of antigen, Ig<sup>HEL</sup>-transgenic B cells localized in follicles, consistent with previous findings that T-zone chemokines and CCR7 are not necessary for follicle formation. However, HEL antigen exposure failed to cause redistribution of

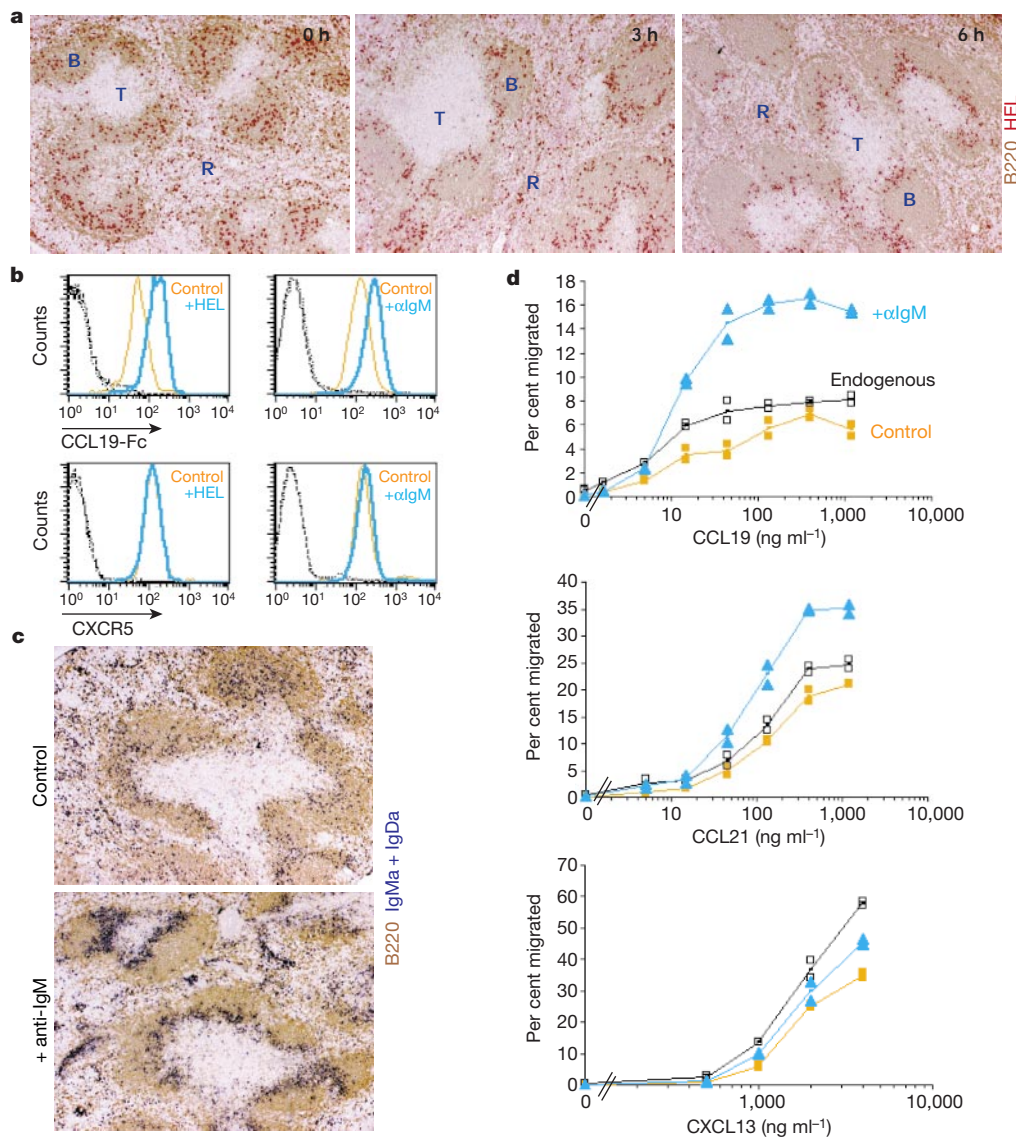


**Figure 1** Antigen-engaged B cells upregulate CCR7, increase responsiveness to T-zone chemokines and migrate to the outer T zone. **a**, Mice that received Ig<sup>HEL</sup>-transgenic B cells were injected with HEL, and the distribution in the spleen of HEL-binding cells (red) and total B cells (brown) was determined 0, 3 and 6 h later. B, B zone; T, T zone; R, red pulp. **b**, CCL19-Fc and CXCR5 staining of Ig<sup>HEL</sup>-transgenic B cells isolated from mice 6 h after saline (control) or HEL injection (left panels), or IgM<sup>a</sup> non-transgenic B cells isolated 5.5 h after transfer of cells that had been incubated *in vitro* in the absence (control) or presence of anti-IgM ( $\alpha$ -IgM; right panels). Blue line, stimulated cells; orange line, control cells; dotted and dashed black lines, control or stimulated cells stained with human LFA3-Fc

(upper panels) or without primary antibody (lower panels) as controls. **c**, Distribution of IgM<sup>a</sup> B cells incubated for 1 h without (control) or with anti-IgM at 5.5 h after transfer to IgM<sup>b</sup> B6 recipient mice. Spleen sections were stained for IgM<sup>a</sup> and IgD<sup>a</sup> (blue stain) to detect transferred B cells, and for B220 (brown) to delineate B-cell follicles. **d**, *Ex vivo* chemotaxis assays of spleen cells from transfer recipient mice. The percentage of input B cells of the indicated type that migrated in response to chemokine is shown in duplicate. The response of stimulated cells to CCL19 and CCL21 was significantly greater than the response of control cells (CCL19,  $P < 0.01$ ; CCL21,  $P < 0.05$ ). Data in **a–d** are representative of more than 3 experiments of each type.

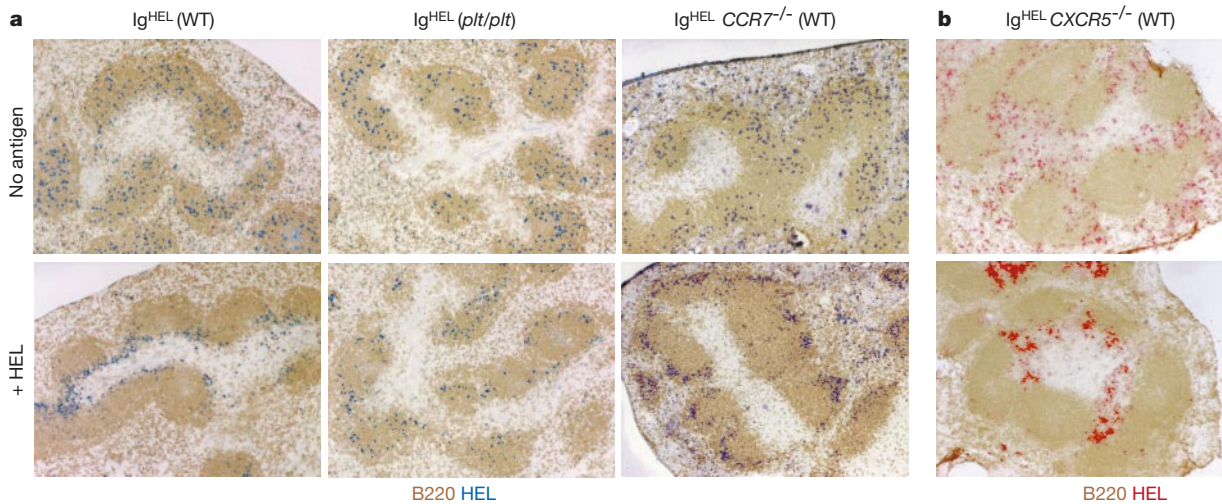


**Figure 2** Localization of antigen-engaged B cells along the B/T boundary is dependent on both T- and B-zone chemokines. **a**, Spleen sections of wild-type (WT) or *plt/plt* mice that received wild-type or *CCR7*<sup>-/-</sup> Ig<sup>HEL</sup>-transgenic B cells, as indicated, 6 h after injection of saline (no antigen) or HEL antigen, stained to detect HEL-binding B cells (blue) and total

B cells (brown). **b**, Spleen sections of wild-type mice that received *CXCR5*<sup>-/-</sup> Ig<sup>HEL</sup>-transgenic B cells, prepared and stained as in **a**, except HEL-binding cells are red. Data are representative of more than 10 experiments for *plt/plt* recipients, three for *CCR7*<sup>-/-</sup> cells, and four for *CXCR5*<sup>-/-</sup> cells.

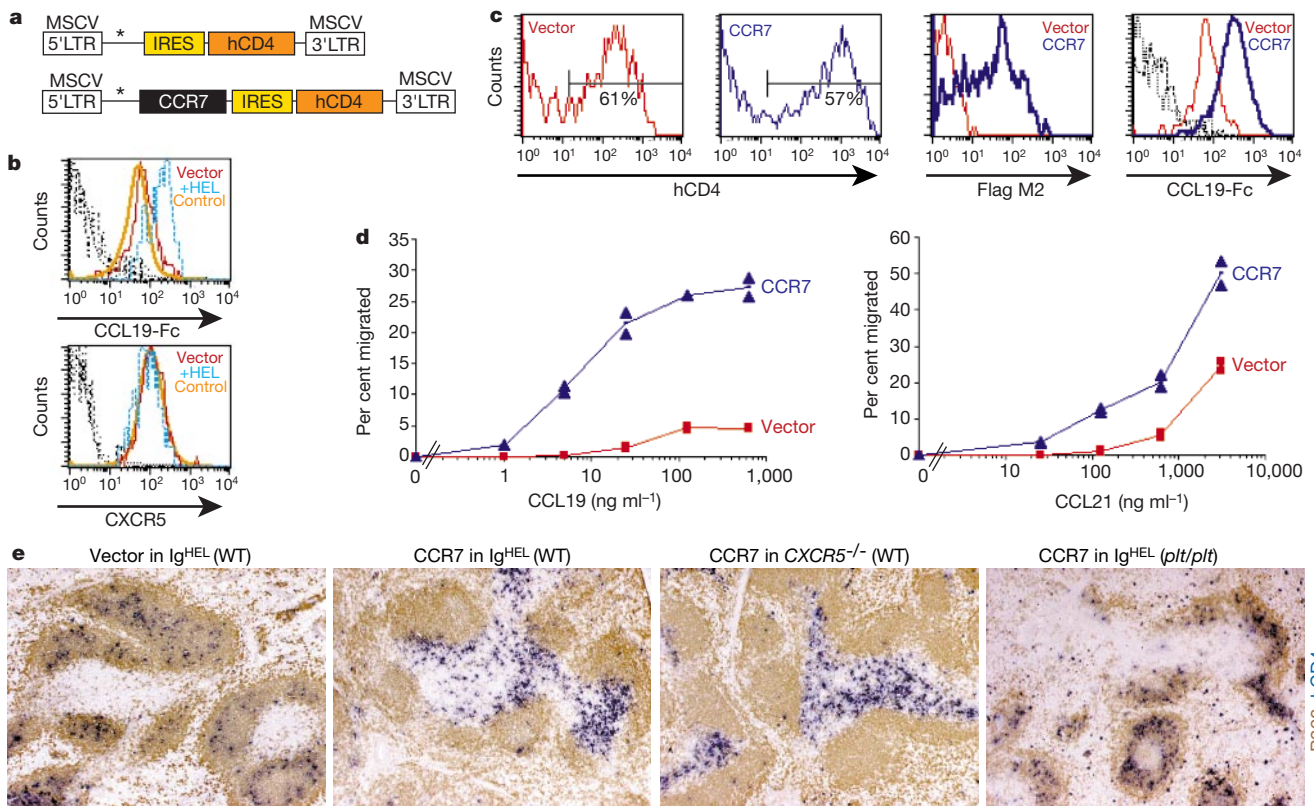


**Figure 3** Increased expression of CCR7 is sufficient to mediate B-cell redistribution to the T zone. **a**, Diagram of the MSCV.2 retroviral vector and Flag-CCR7-containing vector. MSCV, murine stem cell virus; LTR, long-term repeat; asterisk, packaging signal; IRES, internal ribosomal entry site; hCD4, cytoplasmic-domain-truncated human CD4. **b**, *Ex vivo* flow cytometric analysis of cells from recipient mice of CFSE-labelled Ig<sup>HEL</sup>-transgenic B cells. CD40-mediated activation and retroviral infection do not alter CCL19-Fc staining or CXCR5 levels. Red line, vector-infected cells from mice lacking HEL; dashed blue line, vector-infected cells from mice injected with HEL; orange line, endogenous B cells; dotted and dashed black lines, staining controls for above cells (see Fig. 1b). **c**, *Ex vivo* flow cytometric analysis of cells from recipient mice of CFSE-labelled Ig<sup>HEL</sup>-transgenic B cells transduced with empty (vector) or Flag-CCR7-containing (CCR7) retroviral vectors. The fraction of transferred B cells expressing human CD4 (two left panels), and Flag-epitope

(Flag M2) and CCL19-Fc staining of the human CD4-positive cells (two right panels), is shown. Blue line, CCR7-infected cells; red line, vector-infected cells; dotted and dashed black lines, control-infected cells or CCR7-infected cells, respectively, stained with human LFA3-Fc as staining control. **d**, *Ex vivo* chemotaxis assays with spleen cells of mice that had received, one day before, Ig<sup>HEL</sup>-transgenic B cells transduced with the indicated retrovirus. The percentage of input B220<sup>+</sup> human CD4<sup>+</sup> control- (vector) or CCR7-infected cells that migrated to the indicated chemokine, is shown. **e**, Spleen distribution of transferred Ig<sup>HEL</sup>-transgenic wild-type (WT) or *CXCR5*<sup>-/-</sup> B cells infected with empty (vector) or CCR7-containing virus, stained to detect transduced cells (human CD4, blue) in relation to B-cell follicles (B220, brown), one day after transfer to wild-type or *plt/plt* recipient mice, as indicated. Data in **b–e** are representative of at least three separate experiments.

cells to the outer T zone (Fig. 2a), indicating a role for CCL19 and/or CCL21. A concern with this approach was that the effect could be indirect, owing to alterations in the T zone that were downstream of T-zone chemokine deficiency. To test for an intrinsic requirement for CCR7 in antigen-engaged B cells, we introduced the Ig<sup>HEL</sup> transgenes onto the CCR7 knockout background<sup>8</sup>, and performed a similar transfer experiment. HEL-binding CCR7-deficient B cells failed to localize in the outer T zone (Fig. 2a); notably, the antigen-engaged CCR7-deficient B cells often moved in the opposite direction, lodged in the pole of the follicle distal to the T-zone.

The flow cytometric and *ex vivo* chemotaxis analyses of antigen-stimulated B cells established that the cells retain CXCR5 expression and responsiveness to CXCL13 (Fig. 1). To examine whether CXCL13 responsiveness influenced the distribution of antigen-binding B cells, CXCR5<sup>-/-</sup> Ig<sup>HEL</sup>-transgenic B cells were transferred to mice in the absence or presence of the HEL antigen. As described previously<sup>13,14</sup>, CXCR5-deficient cells did not enter follicles, and many of the cells were found in the red pulp, with some cells localized at entry points (bridging zones) to the T-cell areas (Fig. 2b). Antigen binding caused a marked increase in the accumulation of cells at the edge of the T zone, confirming that CXCR5 is not required for cells to move to this compartment in response to antigen (Fig. 2b). However, the CXCR5-deficient cells failed to distribute uniformly along the B/T boundary, and were found more often in clusters near bridging zones (Fig. 2b). Therefore, CXCL13 influences the localization of antigen-engaged B cells,

helping to distribute the cells along the B/T boundary.

The above findings suggested that the increased surface expression of CCR7 induced by BCR signalling might be the principal determinant causing B-cell relocalization to the T zone. To test this model, we used retroviral-mediated gene transfer<sup>15-17</sup> to selectively alter chemokine receptor levels in B cells, followed by adoptive transfer into mice (Fig. 3). To activate the B cells for retroviral infection, we incubated Ig<sup>HEL</sup>-transgenic cells with mitogenic doses of anti-CD40 antibody. In contrast to BCR triggering, cells activated by CD40 remain competent for migration into follicles, and do not undergo major changes in expression of CXCR5 or CCR7 (Fig. 3b). As expected, transduction with Flag-tagged retrovirus containing CCR7 led to co-expression of the marker protein—cytoplasmic-domain-truncated human CD4 (Fig. 3a)—and Flag-CCR7 on the surface of most of the transferred B cells (Fig. 3c), and increased CCL19-Fc binding by these cells (Fig. 3c). *Ex vivo* chemotaxis analysis of the transduced cells revealed that the higher CCR7 expression conferred an increase in sensitivity to CCL19 and CCL21 (Fig. 3d). This outcome was similar to the effect of BCR stimulation (Fig. 1d), although of a greater magnitude, consistent with the higher expression of CCR7 on retrovirally transduced cells (four–fivefold increase) compared with BCR-stimulated cells (two–threefold increase). Using human CD4 staining as a surrogate marker for tracking B cells that overexpress CCR7 *in situ*, we found that the cells distributed within the T zone and failed to localize within B-cell follicles (Fig. 3e). By

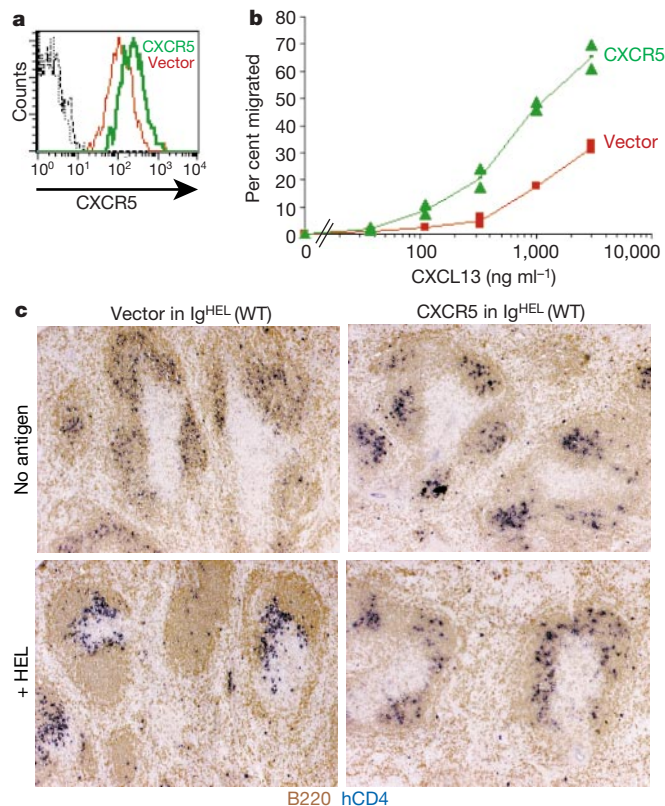


**Figure 4** Overexpression of CXCR5 is sufficient to override antigen-induced B-cell movement to the T-cell zone. **a**, *Ex vivo* flow cytometric analysis of spleen cells from recipient mice of CFSE-labelled Ig<sup>HEL</sup>-transgenic B cells transduced with empty or CXCR5-containing retroviral vector. Green line, CXCR5-infected cells; red line, vector-infected cells; dotted and dashed black lines, control-infected cells or CXCR5-infected cells, respectively, stained without primary antibody as staining control. **b**, *Ex vivo* chemotaxis assays with spleen cells of mice that, one day earlier, had received Ig<sup>HEL</sup>-transgenic B

cells transduced with the indicated retrovirus. Assays were as in Fig. 3. **c**, Distribution in spleen of transferred Ig<sup>HEL</sup>-transgenic wild-type (WT) cells that had been infected with empty (vector) or CXCR5-containing virus, and transferred to wild-type mice that, one day later, received an injection of saline or HEL antigen, as indicated. Tissue was isolated 7 h later and stained to detect human CD4 (blue) and B220 (brown). Data in **a–c** are representative of three separate experiments.

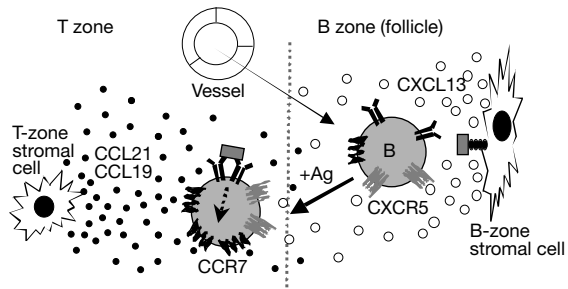


**Figure 5** Schematic representation of the mechanism for B-cell movement to the B/T boundary after BCR engagement. B cells enter spleen and lymph nodes through blood vessels that are mostly located outside B-cell zones. Naive B cells express high levels of CXCR5 and low levels of CCR7, and their responsiveness to the CXCR5 ligand, CXCL13, dominates, causing them to move into follicles. When antigen is encountered, BCR signalling leads to increased surface CCR7 and increased responsiveness to the CCR7 ligands, CCL19 and CCL21. The shifted balance of chemokine responsiveness causes the antigen-engaged cell to move to the T zone. Open circles, CXCL13; filled circles, CCL19 or CCL21; rectangular box, antigen; antigen-retaining structure on stromal cell, complement receptor; Y-shaped structure on B cell, BCR.

contrast, cells transduced with the empty vector localized within follicles in a similar way to non-transduced cells (Fig. 3e). The CCR7-transduced B cells accumulated frequently along the B/T boundary in greater numbers than in other parts of the T zone (Fig. 3e). This effect was not seen when the CCR7-transduced cells lacked CXCR5 (Fig. 3e), establishing that accumulation near the boundary was dependent on responsiveness to CXCL13. As expected, movement of CCR7-transduced B cells to the T zone was dependent on CCL19 and/or CCL21, as the cells failed to lodge in this zone in *plt/plt* mice (Fig. 3e).

Antigen-engaged B cells are responsive to both T- and B-zone chemokines, and the findings shown in Figs 2 and 3 indicate that responsiveness to both types of chemokine contribute towards positioning the cells. To further explore the extent to which antigen-engaged B-cell positioning reflects the outcome of a balance of chemokine responsiveness, we tested whether overexpression of CXCR5 by retroviral transduction (Fig. 4a) is sufficient to overcome the effect of antigen engagement on B-cell distribution. Adoptively transferred cells overexpressing CXCR5 showed a marked increase in responsiveness to CXCL13 in *ex vivo* chemotaxis assays (Fig. 4b). BCR engagement failed to promote follicular exclusion of cells overexpressing CXCR5, and the cells were found in follicles, within the zone of CXCL13 expression (Fig. 4c and data not shown). Cells transduced with empty vector were excluded from follicles in a manner similar to non-transduced cells (Fig. 4c).

These findings establish that the positioning of B cells in lymphoid tissues *in vivo* is determined by the relative responsiveness of the cells to chemokines made in separate but adjacent zones. In naive B cells, the balance of responsiveness is in favour of CXCL13, and the cells migrate into follicles. Upon antigen encounter and BCR stimulation, a change in the balance occurs that favours the response to T-zone chemokines, and this change is sufficient to redistribute antigen-engaged B cells to the T zone (Fig. 5). Our observations suggest that B cells integrate signals from two chemokine receptors simultaneously, consistent with *in vitro* studies showing that neutrophils can sense and respond to two sources of chemoattractant<sup>18</sup>. Antigen-stimulated B cells respond less strongly than T cells and dendritic cells to CCL19 and CCL21 (refs 19, 20), and we propose that this contributes to their exclusion from the central T zone. Reduced CCR7 expression in T-helper subtype 2 cell lines has been associated with the failure of these cells to reach the central T zone<sup>17</sup>. The possible contribution of additional factors, such as adhesion molecules, to placement of antigen-engaged B cells

at the B/T boundary are not ruled out by our study. In addition, although we have focused on the behaviour of B cells in response to foreign antigen, autoreactive B cells that are chronically engaged by auto-antigen also lodge at the B/T boundary before their elimination<sup>21,22</sup>. It is probable that a similar mechanism operates to regulate the localization of auto-antigen-binding cells. We suggest that the positioning of many cell types is determined by balanced responsiveness to chemoattractants emanating from adjacent zones. This mechanism may be used in the positioning of other types of leukocytes, such as activated T cells and subsets of dendritic cells<sup>3,17,23</sup>, in the localization of growing axons, and in the patterning of organs during development<sup>24</sup>. □

## Methods

### Mice, adoptive cell transfer and stimulation procedures

Ig<sup>HEL</sup>-transgenic mice were of the MD4 line<sup>6</sup>, *plt/plt* mice<sup>25</sup> on a BALB/c background were crossed to C57BL/6 (B6) mice for six generations; *CXCR5*<sup>-/-</sup> mice<sup>13</sup> were eighth-generation backcrossed to B6 mice, and *CCR7*<sup>-/-</sup> mice<sup>8</sup> were on a mixed B6/129 background. Igha (Ig heavy chain of a) Thy1a Gpi1a B6 mice (termed IgM<sup>d</sup> congenic B6) were from Jackson Laboratory. B6 (IgM<sup>b</sup>) recipient mice were from Charles River or a colony maintained at University of California San Francisco. To provide *CCR7*<sup>-/-</sup> cells for adoptive transfer, lethally irradiated B6 mice were reconstituted for five weeks with *CCR7*<sup>-/-</sup> Ig<sup>HEL</sup> bone marrow, as described<sup>2</sup>. Adoptive transfers were performed using 1.5–3 × 10<sup>7</sup> spleen cells per recipient mouse<sup>2</sup>. In some experiments, mice were injected intraperitoneally 12–18 h after the cell transfer with 0.8–1 mg HEL (Sigma) in phosphate-buffered saline (PBS) or with PBS alone. For IgM stimulation, splenocytes were cultured for 1 h at 37 °C in RPMI 1640 supplemented with 3% FBS, 50 µg ml<sup>-1</sup> streptomycin, 50 U ml<sup>-1</sup> penicillin, 10 mM HEPES with or without 10 µg ml<sup>-1</sup> goat anti-mouse IgM F(ab')<sub>2</sub> polyclonal antibodies (Jackson ImmunoResearch), washed and then transferred. Spleens were collected 5.5–6 h after stimulation or at the time indicated in the results, and cut into fragments with 1 out of 3 being used to generate cell suspensions for *ex vivo* flow cytometry and chemotaxis assays, and 2 out of 3 being frozen in OCT compound (Sakura).

### Retroviral transduction of B cells

Flag-tagged CCR7 (ref. 19) or CXCR5 (ref. 26) were cloned into the MSCV2.2 retroviral vector containing cytoplasmic-domain-truncated human CD4 as an expression marker downstream of the internal ribosomal entry site (IRES)<sup>17</sup>. Retrovirus containing supernatant was generated using the Bosc23 packaging cell line together with pCL-Eco packaging vector<sup>27</sup>, as described<sup>28</sup>. For B-cell activation, Ig<sup>HEL</sup>-transgenic or *CXCR5*<sup>-/-</sup> Ig<sup>HEL</sup>-transgenic mice were injected intraperitoneally with 4–6 mg HEL, splenocytes were collected after 6–8 h, cultured in RPMI 1640 supplemented with 10% FBS, 2 mM L-glutamine, 50 µg ml<sup>-1</sup> streptomycin, 50 U ml<sup>-1</sup> penicillin, 10 mM HEPES, and 50 µM 2-ME in the presence of 10 µg ml<sup>-1</sup> anti-CD40 monoclonal antibody (clone FGK45, a gift from A. Rolink), and spin-infected 24 h later with retroviral supernatants and 4 µg ml<sup>-1</sup> polybrene (Sigma). Two days after infection, cells were collected, in some experiments labelled with 2 µM CFSE, and adoptively transferred into mice. In all experiments, between 45% and 75% of B cells were retrovirally transduced as assessed by flow cytometric analysis for human CD4 expression. T cells were not activated by the antigen and anti-CD40 treatment, and were not detectably infected by the retroviruses.

### Chemotaxis assays, flow cytometry and immunohistochemistry

For chemotaxis assays, cells transmigrated across 5-µm transwell filters (Corning Costar Corp) for over 3 h in response to a stimulus in the bottom chamber, and were enumerated by flow cytometry<sup>19</sup>. Chemokines were provided by R&D Systems. Transwell assays were performed in duplicate for each chemokine concentration, and were repeated using cells from a minimum of three different animals of each type. We carried out statistical analyses using the paired *t*-test. The CCL19-Fc recombinant protein was a fusion of mouse CCL19 and the human IgG1 constant region<sup>29</sup>. For control staining, we used human LEA3-Fc (a gift from J. Browning). Antibodies used were anti-CXCR5 (refs 13, 30), anti-human CD4-phycoerythrin (BD PharMingen), and biotinylated Flag M2 (Sigma). We analysed labelled cells on a FACSCaliber (Becton Dickinson). See Supplementary Information for CCL19-Fc background staining on *CCR7*<sup>-/-</sup> cells, and anti-CXCR5 background staining on *CXCR5*<sup>-/-</sup> B cells. Immunohistochemical analysis was performed as described<sup>14</sup>, with the exception that HEL-binding cells were detected by incubation with 1–5 µg ml<sup>-1</sup> HEL antigen followed by biotin-conjugated rabbit anti-HEL (Rockland). Human CD4 was detected with biotin-conjugated mouse anti-human CD4 (BD PharMingen). Biotinylated antibodies were visualized with alkaline phosphatase-conjugated streptavidin (Jackson ImmunoResearch) and Fast Red TR or Fast Blue BB salt (Sigma) as a substrate. All images of spleen sections were obtained at × 5 objective magnification, and each image shown is representative of all (10–20) white pulp cords observed in three transverse sections of each spleen.

Received 8 November 2001; accepted 10 January 2002.

1. Liu, Y.-J., Oldfield, S. & MacLennan, I. C. M. Memory B cells in T cell-dependent antibody responses colonize the splenic marginal zones. *Eur. J. Immunol.* **18**, 355–362 (1988).
2. Cyster, J. G. & Goodnow, C. C. Antigen-induced exclusion from follicles and anergy are separate and complementary processes that influence peripheral B cell fate. *Immunity* **3**, 691–701 (1995).

3. Garside, P. *et al.* Visualization of specific B and T lymphocyte interactions in the lymph node. *Science* **281**, 96–99 (1998).
4. Cyster, J. G. Chemokines and cell migration in secondary lymphoid organs. *Science* **286**, 2098–2102 (1999).
5. Zlotnik, A. & Yoshie, O. Chemokines: a new classification system and their role in immunity. *Immunity* **12**, 121–127 (2000).
6. Goodnow, C. C. *et al.* Altered immunoglobulin expression and functional silencing of self-reactive B lymphocytes in transgenic mice. *Nature* **334**, 676–682 (1988).
7. Gunn, M. D. *et al.* Mice lacking expression of secondary lymphoid organ chemokine have defects in lymphocyte homing and dendritic cell localization. *J. Exp. Med.* **189**, 451–460 (1999).
8. Förster, R. *et al.* CCR7 coordinates the primary immune response by establishing functional microenvironments in secondary lymphoid organs. *Cell* **99**, 23–33 (1999).
9. Basten, A. *et al.* Self tolerance in the B cell repertoire. *Immunol. Rev.* **122**, 5–19 (1991).
10. Luther, S. A., Tang, H. L., Hyman, P. L., Farr, A. G. & Cyster, J. G. Coexpression of the chemokines ELC and SLC by T zone stromal cells and deletion of the ELC gene in the *plt/plt* mouse. *Proc. Natl Acad. Sci. USA* **97**, 12694–12699 (2000).
11. Nakano, H. & Gunn, M. D. Gene duplications at the chemokine locus on mouse chromosome 4: multiple strain-specific haplotypes and the deletion of secondary lymphoid-organ chemokine and EBI-1 ligand chemokine genes in the *plt* mutation. *J. Immunol.* **166**, 361–369 (2001).
12. Vassileva, G. *et al.* The reduced expression of 6CKine in the *plt* mouse results from the deletion of one of two 6CKine genes. *J. Exp. Med.* **190**, 1183–1188 (1999).
13. Förster, R. *et al.* A putative chemokine receptor, BLR1, directs B cell migration to defined lymphoid organs and specific anatomic compartments of the spleen. *Cell* **87**, 1037–1047 (1996).
14. Ansel, K. M. *et al.* A chemokine driven positive feedback loop organizes lymphoid follicles. *Nature* **406**, 309–314 (2000).
15. Ouyang, W. *et al.* Inhibition of Th1 development mediated by GATA-3 through an IL-4-independent mechanism. *Immunity* **9**, 745–755 (1998).
16. Van Parijs, L., Refaeli, Y., Abbas, A. K. & Baltimore, D. Autoimmunity as a consequence of retrovirus-mediated expression of C-FLIP in lymphocytes. *Immunity* **11**, 763–770 (1999).
17. Randolph, D. A., Huang, G., Carruthers, C. J. L., Bromley, L. E. & Chaplin, D. D. Differential expression of CCR7 on Th1 and Th2 cells: Importance in control of T cell localization and delivery of help for antibody responses *in vivo*. *Science* **286**, 2159–2162 (1999).
18. Foxman, E. F., Kunkel, E. J. & Butcher, E. C. Integrating conflicting chemotactic signals. The role of memory in leukocyte navigation. *J. Cell Biol.* **147**, 577–588 (1999).
19. Ngo, V. N., Tang, H. L. & Cyster, J. G. Epstein–Barr virus-induced molecule 1 ligand chemokine is expressed by dendritic cells in lymphoid tissues and strongly attracts naive T cells and activated B cells. *J. Exp. Med.* **188**, 181–191 (1998).
20. Kellermann, S. A., Hudak, S., Oldham, E. R., Liu, Y. J. & McEvoy, L. M. The CC chemokine receptor-7 ligands 6CKine and macrophage inflammatory protein-3 beta are potent chemoattractants for *in vitro*- and *in vivo*-derived dendritic cells. *J. Immunol.* **162**, 3859–3864 (1999).
21. Cyster, J. G., Hartley, S. B. & Goodnow, C. C. Competition for follicular niches excludes self-reactive cells from the recirculating B-cell repertoire. *Nature* **371**, 389–395 (1994).
22. Mandik-Nayak, L., Bui, A., Noorchashm, H., Eaton, A. & Erikson, J. Regulation of anti-double-stranded DNA B cells in nonautoimmune mice: localization to the T–B interface of the splenic follicle. *J. Exp. Med.* **186**, 1257–1267 (1997).
23. Iwasaki, A. & Kelsall, B. L. Localization of distinct Peyer's patch dendritic cell subsets and their recruitment by chemokines macrophage inflammatory protein (MIP)-3α, MIP-3β, and secondary lymphoid organ chemokine. *J. Exp. Med.* **191**, 1381–1394 (2000).
24. Belloch, R., Newman, C. & Kimble, J. Control of cell migration during *Caenorhabditis elegans* development. *Curr. Opin. Cell Biol.* **11**, 608–613 (1999).
25. Nakano, H. *et al.* Genetic defect in T lymphocyte-specific homing into peripheral lymph nodes. *Eur. J. Immunol.* **27**, 215–221 (1997).
26. Gunn, M. D. *et al.* A B-cell-homing chemokine made in lymphoid follicles activates Burkitt's lymphoma receptor-1. *Nature* **391**, 799–803 (1998).
27. Naviaux, R. K., Costanzi, E., Haas, M. & Verma, I. M. The pCL vector system: rapid production of helper-free, high-titer, recombinant retroviruses. *J. Virol.* **70**, 5701–5705 (1996).
28. Pear, W. S., Nolan, G. P., Scott, M. L. & Baltimore, D. Production of high-titer helper-free retroviruses by transient transfection. *Proc. Natl Acad. Sci. USA* **90**, 8392–8396 (1993).
29. Hargreaves, D. C. *et al.* A coordinated change in chemokine responsiveness guides plasma cell movements. *J. Exp. Med.* **194**, 45–56 (2001).
30. Schmidt, K. N., Hsu, C. W., Griffin, C. T., Goodnow, C. C. & Cyster, J. G. Spontaneous follicular exclusion of SHP1-deficient B cells is conditional on the presence of competitor wild-type B cells. *J. Exp. Med.* **187**, 929–937 (1998).

Supplementary Information accompanies the paper on Nature's website (<http://www.nature.com>).

### Acknowledgements

We thank K. Murphy and W. Sha for retroviral vectors; P. Andres, D. Bhattacharya, Y. Refaeli and W. Sha for advice; M. Matloubian, T. Okada, D. Stainier and A. Weiss for comments on the manuscript; and A. Bidgol for help with screening mice. K.R. was supported by a Human Frontier Science Program Long Term Fellowship and is currently supported by a Leukemia and Lymphoma Society Special Fellowship. E.H.E. is a Howard Hughes Medical Institute (HHMI) predoctoral fellow, and J.G.C. is a HHMI assistant investigator and a Packard Fellow. This work was supported in part by a grant from the National Institutes of Health.

### Competing interests statement

The authors declare that they have no competing financial interests.

Correspondence and requests for materials should be addressed to J.G.C. (e-mail: [cyster@itsa.ucsf.edu](mailto:cyster@itsa.ucsf.edu)).

## Ubiquitination-dependent cofactor exchange on LIM homeodomain transcription factors

Heather P. Ostendorff<sup>\*,†</sup>, Reto I. Peirano<sup>\*,†</sup>, Marvin A. Peters<sup>\*</sup>, Anne Schlüter<sup>\*</sup>, Michael Bossenz<sup>\*</sup>, Martin Scheffner<sup>‡</sup> & Ingolf Bach<sup>\*</sup>

<sup>\*</sup>Zentrum für Molekulare Neurobiologie Hamburg (ZMNH), Universität Hamburg, Martinistrasse 85, 20251 Hamburg, Germany  
<sup>‡</sup>Institut für Biochemie I, Medizinische Fakultät, Universität zu Köln, Joseph-Stelzmann-Strasse 52, 50931 Köln, Germany  
<sup>†</sup>These authors contributed equally to this work

The interactions of distinct cofactor complexes with transcription factors are decisive determinants for the regulation of gene expression. Depending on the bound cofactor, transcription factors can have either repressing or transactivating activities<sup>1</sup>. To allow a switch between these different states, regulated cofactor exchange has been proposed<sup>2,3</sup>; however, little is known about the molecular mechanisms that are involved in this process. LIM homeodomain (LIM-HD) transcription factors associate with RLIM (RING finger LIM domain-binding protein) and with CLIM (cofactor of LIM-HD proteins; also known as NLI, Ldb and Chip) cofactors. The co-repressor RLIM inhibits the function of LIM-HD transcription factors, whereas interaction with CLIM proteins is important for the exertion of the biological activity conferred by LIM-HD transcription factors<sup>4,5</sup>. Here we identify RLIM as a ubiquitin protein ligase that is able to target CLIM cofactors for degradation through the 26S proteasome pathway. Furthermore, we demonstrate a ubiquitination-dependent association of RLIM with LIM-HD proteins in the presence of CLIM cofactors. Our data provide a mechanistic basis for cofactor exchange on DNA-bound transcription factors, and probably represent a general mechanism of transcriptional regulation.

We have used the regulation of LIM-HD transcription factors<sup>4,5</sup> as a model system to investigate mechanisms of controlling transcription factor activity. Their interaction with CLIM cofactors is thought to be critical for the exertion of the transcriptional and biological activity of this class of developmental regulators<sup>6–11</sup>. In contrast, LIM-HD protein activity is negatively regulated by nuclear LIM-only (LMO) cofactors<sup>9,10,12</sup>—which compete with LIM-HD proteins for CLIM cofactors—and by the RING H2 zinc finger protein RLIM. Indeed, overexpression of full-length RLIM or a dominant negative version of CLIM (DN-CLIM) in the developing chick wing results in very similar phenotypes, inhibiting the development of distal wing structures<sup>8</sup>.

The ubiquitin proteasome-dependent proteolytic pathway is involved in the regulation of critical developmental regulator proteins such as NF-κB, c-Jun, Tramtrack<sup>13</sup> and OBF-1/BOB.1 (refs 14, 15). As RLIM contains a RING H2 zinc finger motif that is often found in ubiquitin protein ligases<sup>16,17</sup>, we tested whether RLIM mediates E2-dependent ubiquitination of itself *in vitro*, as has been shown for other RING finger proteins<sup>18</sup>. Indeed, RLIM was ubiquitinated in the presence of the E2 ubiquitin-conjugating enzyme UbcH5 (Fig. 1a). This reaction was dependent on the RING finger because RING-finger-deleted or mutated versions of RLIM protein (RLIMΔRING and RLIMΔ9, respectively; see Methods) were no longer ubiquitinated by UbcH5 (Fig. 1b). As RLIM binds to nuclear LIM proteins and to CLIM cofactors<sup>8</sup>, we examined whether RLIM could serve as a ubiquitin protein ligase for these proteins. Whereas, under the conditions used, bacterially expressed full-length RLIM was not able, or only weakly able, to ubiquitinate the LIM-HD transcription factors Lhx1, Lhx3 and Isl1,